Journal of the Taiwan Institute of Chemical Engineers 44 (2013) 622–629

Contents lists available at SciVerse ScienceDirect

Journal of the Taiwan Institute of Chemical Engineers

journal homepage: www.elsevier.com/locate/jtice

Rice husk ash as a catalyst precursor for biodiesel production

Kung-Tung Chen [b], Jian-Xun Wang [a], Yong-Ming Dai [a], Po-Hsiang Wang [a], Cyong-Ying Liou [c], Chia-Wei Nien [a], Jhong-Syuan Wu [a], Chiing-Chang Chen [a,*]

[a] Department of Science Application and Dissemination, National Taichung University of Education, Taichung 40306, Taiwan
[b] The Teaching Center of Natural Science, Minghsin University of Science and Technology, Hsinchu 30401, Taiwan
[c] Department of Applied Chemistry, Chung Shan Medical University, Taichung 40227, Taiwan

ARTICLE INFO

Article history:
Received 23 August 2012
Received in revised form 1 January 2013
Accepted 6 January 2013
Available online 13 March 2013

Keywords:
Biodiesel
Rice husk ash
Heterogeneous catalyst
Transesterification
Soybean oil

ABSTRACT

The transesterification of soybean oil with methanol was carried out in the presence of Li-modified rice husk ash catalyst at atmospheric pressure. The catalyst was prepared using a simple solid-state reaction, mixing, and well grinding 1.00 g RHA with 1.23 g Li_2CO_3 calcined at 900 °C in air for 4 h. The catalysts were characterized using XRD, SEM, FTIR, TGA-DTA, and the Hammett indicator. The XRD peaks were mainly consistent with Li_2SiO_3. The catalyst was highly active because its basic strength (H_) exceeded 15.0. The catalyst was also air-insensitive, as only a few CO_3^{2-} anions formed on the surface of catalyst after exposure to air for 72 h, and no obvious LiOH formed on the catalyst surface. Under the optimal reaction conditions of a methanol/oil molar ratio of 24:1, a 4% catalyst amount, and a reaction temperature of 65 °C for 3 h, this approach achieved 99.5% conversion to biodiesel.

1. Introduction

Biodiesel has recently attracted attention as a renewable biofuel with fewer pollutant emissions than mineral diesel upon combustion [1–3]. Heterogeneous catalysts have the advantage that they can be easily removed from the reaction mixture by filtration and recycled [4]. One way to reduce the cost of the catalysts is to use agricultural wastes as catalytic materials. In addition to reducing the cost of procuring and synthesizing the catalytic material, this approach creates additional revenue opportunities for farmers. Using waste materials as catalysts (instead of discarding them) also reduces the cost of waste handling and disposal. The waste materials used as heterogeneous catalysts studied so far include waste oyster shell [5,6], Turbonilla striatula shell [7], cockle shell [8], mussel shell [9], mollusk shell [10], egg shell [11], mud crab shell [12], Meretrix shell [13], and snail shell [14].

Rice covers 1% of the earth's surface and is a primary source of food for billions of people [15]. Rice husk is the outer cover of the rice, and accounts for approximately 20% of paddy production, based on weight. The main characteristics of rice husk include a 16.3 MJ/kg heating value, a content of 74.0% volatile matter, and 12.8% ash [16]. These characteristics indicate that the rice husk could be a good solid fuel for burning in a boiler to produce steam in various industries [17], and thus conserving both energy and resources. The burning of rice husk in air always produces rice husk ash (RHA), which is typically viewed as agricultural waste [18]. Each ton of rice produces 200 kg of rice-husks, which upon complete combustion produce 40 kg of RHA. No other crop by-product generates a greater quantity of ash when it is burnt [19]. RHA is largely composed of silica (87–99%) with small amounts of inorganic salts [20,21]. About 70 million tons of RHA is produced annually worldwide and adequate alternative dispositions must be planned to avoid negative environmental effects. RHA has been widely used as a construction material in concrete [15,22], or as an adsorbent to adsorb organic dye, such as malachite green [23], and inorganic metal such as $Pd^{2+}$and Cu^{2+} metal ions [24,25]. Because of its high silica content, RHA can be an economically viable raw material for producing silicates and silica in recent years [26,27]. Some researchers have used RHA to synthesize ZSM-5 zeolite [25] or NaY [28].

Waste shells can be used as a catalyst and source of CaO, which adds value to the generated waste. Calcium oxide (CaO) is a promising basic heterogeneous catalyst for synthesizing biodiesel at mild temperatures (below the boiling point of methanol) and at atmospheric pressure [29], but it is rapidly hydrated and carbonated upon contact with room temperature air. A few minutes are adequate for CaO to chemisorb a substantial amount of H_2O and CO_2 in atmospheric air [30]. The experiments in this study used RHA as a low-cost material to prepare solid base catalyst

* Corresponding author.
E-mail address: ccchen@ms3.ntcu.edu.tw (C.-C. Chen).

1876-1070/$ – see front matter © 2013 Taiwan Institute of Chemical Engineers. Published by Elsevier B.V. All rights reserved.
http://dx.doi.org/10.1016/j.jtice.2013.01.006

using Li_2CO_3 as an activating agent through a solid state reaction. To the best of our knowledge, this is the first attempt to use silica from RHA as a raw material for biodiesel production. The catalyst was air-insensitive and can be directly used for biodiesel production without further drying or thermal pretreatment. This approach avoids the usual activation of solid catalysts at high temperature.

2. Materials and methods

2.1. Catalyst preparation

Soybean cooking oil (Great Wall Enterprise Co., Taiwan), methanol (ACS grade, ECHO Chemical Co., Miaoli, Taiwan) and reagent grade Li_2CO_3 (Shimakyu's Pure Chemicals, Osaka, Japan) were used as received. Rice husk was obtained from a rice farm in Yunlin, Middle Taiwan.

Dry raw rice husks (RHs) were sieved to eliminate residual rice and clay particles. After thorough washing with deionized water, the RHs were filtered and air-dried at room temperature. A sample of rice husk was converted into rice husk ash by heat-treating rice husk at 900 °C for 4 h. After washing with deionized water and filtration, the RHA was dried at 120 °C for 16 h. Results show that highly active solid catalyst can be obtained by mixing and well grinding 1.00 g RHS with 1.23 g Li_2CO_3 calcined at 900 °C in air for 4 h.

2.2. Reaction procedures

The conversion of soybean oil to biodiesel was performed in a 250 ml flat-bottomed flask, equipped with a reflux condenser and a magnetic stirrer. The reactor was initially filled with 12.5 g of soybean oil, which was heated to 65 °C for 3 h while stirring at 300 rpm. The reactant was stirred evenly to avoid splashing in the flask at the stirring speed. The timing of the reaction was initiated as soon as the mixture of methanol and the catalyst was added into the reactor. The effects of molar ratio of methanol to oil (3:1–24:1), and catalyst/oil weight ratio (1–5 wt.%), on the conversion of triglycerides to biodiesel were investigated. All of the experiments were performed at atmospheric pressure. After the transesterification reaction, DI water was added into the reaction mixture to stop the reaction. The biodiesel and glycerol layers were easily separated due to differing densities, of 0.86 and 1.126 g/cm^3, respectively. A supernatant was filtered through a common filter paper, and then excess methanol and water were evaporated prior to fatty acid methyl ester (FAME) analysis.

2.3. Catalyst characterization

The base strength of as-prepared catalysts (H_) was determined using Hammett indicators [31]. Approximately 50 mg of the sample was shaken with 1 ml methanol solution of the Hammett indicator. 2 h were allowed to elapse for the reaching of equilibrium after which no additional change of color took place. The basic strength was defined as being stronger than the weakest indicator which exhibited a color change, and weaker than the strongest indicator which produced no color change. Bromthymol blue (H_ = 7.2), phenolphthalein (H_ = 9.8), 2,4-dinitroaniline (H_ = 15.0), and 4-nitroaniline (H_ = 18.4) were obtained from Sigma–Aldrich (St. Louis, MO, USA) and used as Hammett indicators at a concentration of 0.02 mol/L. The characterization of as-prepared catalysts was performed using a powder X-ray diffractometer (XRD, MAC MXP18, Tokyo, Japan), with Cu Kα radiation, over a 2θ range from 10 to 80° with a step size of 0.04°, and at a scanning speed of 3° min^{-1}. The microstructures of as-prepared catalysts were observed using a field emission scanning electron microscope (SEM, JEOL JSM-7401F, Tokyo, Japan). For FTIR spectroscopy, samples were analyzed using a Spectrometer NICOLET 380 operating in attenuated total reflection mode (Pike Technologies, GladiATR for FTIR with diamond crystal) at a spectral range of 4000–400 cm^{-1}. The infrared spectra were collected and analyzed using a data acquisition computer and OMNIC 4.1b software (Nicolet Corp.). The background and spectral measurements were averaged against 32 scans with a resolution of 4 cm^{-1}. Thermogravimetric analyses were carried out with a Seiko SSC 5000 instrument. The samples (13.8 mg) were heated from room temperature up to 1000 °C, with a scan rate of 5 °C/min, and under an air atmosphere stream (air flow = 80 ml/min) to ensure water desorption. The samples were analyzed as received (*i.e.* without any vacuum pre-treatment or special heat conditioning).

2.4. Analytical methods

FAME concentrations, expressed as the biodiesel purity of the product, were determined using a gas chromatography system (Thermo trace GC ultra, Thermo Co., Austin, TX, USA), equipped with a flame ionization detector, a capillary column (Tr-biodiesel (F), Thermo Co., 30 m in length with 0.25 mm i.d. and 0.25 μm film thickness), the programmed column oven, and a programmed temperature injector. The oven temperature program consisted of: start at 120 °C (hold 1 min), increase at a rate of 30 °C/min to 220 °C (hold 1 min), then increase at a rate of 10 °C/min to 250 °C (hold 1 min). The temperature of the programmed temperature injector was 90 °C for 0.05 min, programmed to 260 °C, at a rate of 10 °C/min. Nitrogen was used as a carrier gas with a flow-rate of 2 ml/min. Fig. 1(a) shows characterization data of internal standard. Amounts of FAME were calculated using the internal standard (methyl heptadecanoate) method, according to method EN 14103. Fig. 1(b) shows the Chromatogram obtained from GC-FID analysis of biodiesel. The peaks were C16:0, C17:0, C18:0, C18:1, C18:2 and C18:3, respectively. These six peaks were the most common peaks in analyzing methyl esters from gas chromatograph.

For quantitative evaluation of the leaching of solid base catalyst under the reaction conditions, some of the samples taken from the reactor were filtered, and then the residual methanol was evaporated in a rotary evaporator so that the FAME and glycerol were left as separate phases. After evaporation, the dry fraction was treated with 0.1 N hydrochloric acid [32,33]. The resulting solution was analyzed using inductively coupled plasma optical emission spectroscopy (ICP-OES, SPECTRO GENESIS, Kleve, Germany) to determine the Li concentration.

3. Results and discussion

3.1. Catalyst characterization

Fig. 2(a) shows the XRD results of RHA, Li_2CO_3 (JCPDS 87-0728), and as-prepared catalyst (Li_2CO_3/RHA weight ratio of 1.23). The parent material RHA is crystalline and consists of α-cristobalite (JCPDS 89-3434) and tridymite (JCPDS 73-0469). The crystalline phase of the RHA was transformed to the Li_2SiO_3 (JCPDS 74-2145) and a few Li_4SiO_4 (JCPDS 37-1472) phase after solid state synthesis with Li_2CO_3.

Fig. 2(b) shows the XRD patterns of the as-prepared sample, samples exposed to air for 24–72 h and after used. The XRD peaks were mainly consistent with Li_2SiO_3 (JCPDS 74-2145). Similar to Na_2SiO_3 at ambient pressure and temperature, Li_2SiO_3 has an orthorhombic structure whose space group was C-center $Cmc2_1$ space group (no. 36), and lattice parameters were a = 9.380 Å, b = 5.400 Å and c = 4.680 Å.

The intensity of Li_4SiO_4 peaks in the diffractogram was very weak, indicating a low Li_4SiO_4 content in the product. To remove

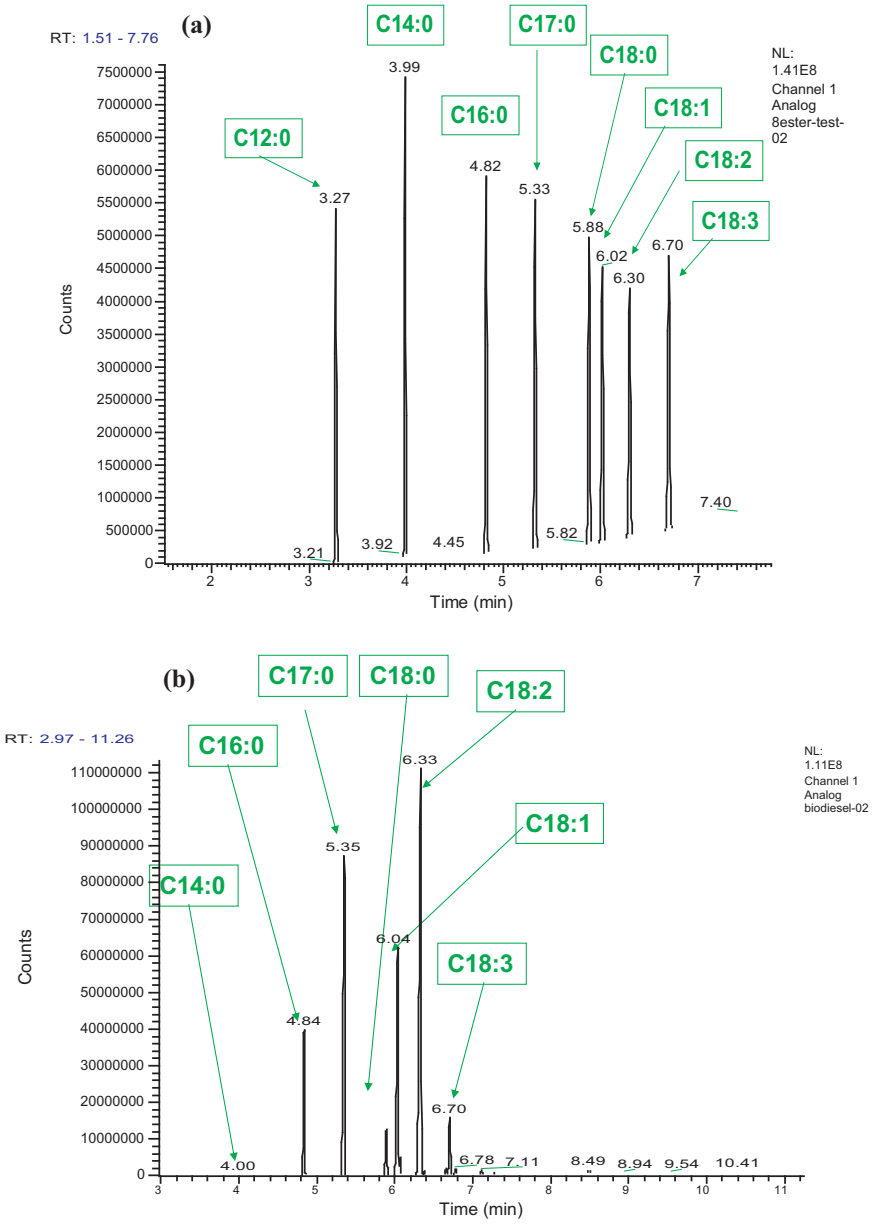

Fig. 1. Chromatogram obtained from GC-FID analysis of (a) internal standard (b) biodiesel.

adsorbed species from the catalyst surface, the reused catalysts were washed with anhydrous methanol and dried at 95 °C (water bath) for 1 h under a vacuum (water-pump suction) prior to XRD and SEM. The crystalline phase of the catalyst stabilized upon exposure to air. It is uncommon for CaO to chemisorb a substantial amount of H_2O quickly in the air and be converted into $Ca(OH)_2$ following a loss of catalytic activity.

Fig. 3(a) shows the FTIR spectra of the as-prepared catalyst synthesized using a solid-state reaction. The bands located at 611, 733, 981, and 1057 cm^{-1} correspond to Si–O–Si bonds [34]. Bands at 1450 and 1483 cm^{-1} were attributed to Li_2CO_3 vibrations [35]. The CO_3^{2-} anions probably formed on the surface of the samples by absorbing CO_2 molecules from the air after calcination. The absorption bands originating from the Si–O– and Li–O– groups were located at 410 and 490 cm^{-1} [34]. The CO_3^{2-} anions formed on the surface of the samples probably by absorbing CO_2 molecules from the air after calcining. The catalyst exposed to air for 72 h and unexposed catalysts had similar FTIR spectra (Fig. 3(b)).

Table 1 shows the basic strength of the as-prepared catalyst, CaO, and Li_2CO_3 after different exposure times to ambient air (temperature 25 ± 2 °C, relative humidity: $50 \pm 5\%$). This study investigates the effects of exposure to air on the catalytic activity of the transesterification reaction. The as-prepared catalyst and CaO appear to have the same initial basic strength. However, the basic strength of CaO decreased significantly following the exposure of the catalysts to air ($7.2 < H_- < 9.8$), thus influencing the conversion to FAME. This deactivation was likely the result of hydration, followed by carbonation on the surface, even after a 3 min exposure to air, when the CaO was appreciably deactivated [36]. This severely limits the practical application of CaO because of its need for an inert atmosphere during handling, storage, reactor loading, and use.

The basic strength (H_-) of catalyst decreased to 9.8–15.0 after exposure to air for 24–72 h. Therefore, slight differences in the soybean oil conversion appeared between the air-exposed catalyst (94.6–87.2%) and the fresh catalyst (97.0%). These results verify that the catalytic sites of as-prepared catalyst were more air-insensitive

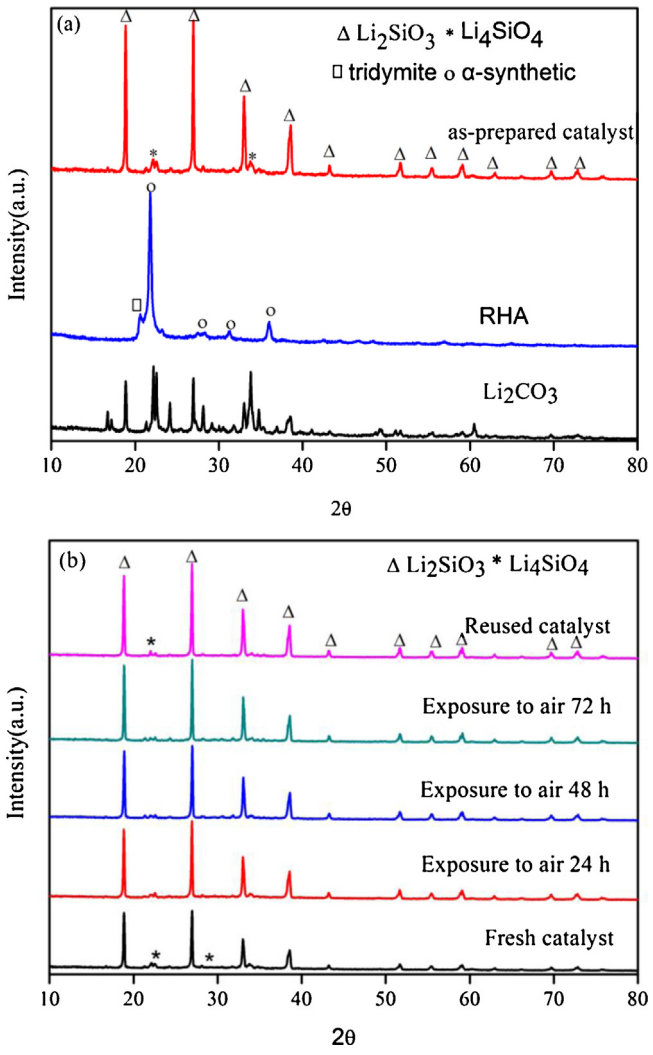

Fig. 2. The XRD patterns of (a) RHA, Li_2CO_3 and as-prepared catalyst (Li_2CO_3/RHA weight ratio of 1.23). (1-tridymite, 2-α-cristobalite), (b) fresh catalyst, catalysts exposed to air for 24–72 h and used catalyst (Li_2CO_3/RHA weight ratio of 1.23). (*Li_4SiO_4).

than CaO. The as-prepared catalyst was a solid base catalyst with the advantage of tolerance to air-exposure, which facilitated the operation of the catalytic reaction.

A reversible reaction between Li_2SiO_3 and CO_2 takes place at temperatures lower than 250 °C [34].

$$Li_2SiO_3 + CO_2 \leftrightarrow Li_2CO_3 + SiO_2\ \Delta E = 115\ \text{KJ/mol} \quad (1)$$

The equilibrium temperature of Li_2SiO_3 was calculated to be 250 °C [37], at which the reaction of CO_2 absorption apparently stops, was calculated from thermodynamics. This is the temperature at which

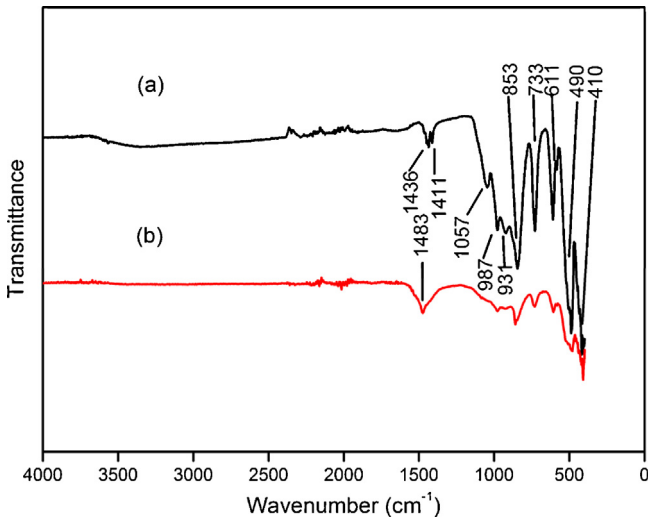

Fig. 3. FTIR spectra of the (a) fresh catalyst and (b) catalyst exposure to air for 72 h.

Gibbs free energy changes (ΔG) for the reaction becomes zero. This is likely because Li_2SiO_3 can absorb CO_2 at temperatures of less than 250 °C, but the absorption rate is very slow in this temperature range from the viewpoint of kinetics [37,38].

Lithium orthosilicate (Li_4SiO_4) has been widely studied as a promising carbon dioxide (CO_2) absorbent [35]. The process of CO_2 capture, using Li_4SiO_4 as a solid absorbent, occurs according to the following reaction [37]:

$$Li_4SiO_{4(s)} + CO_{2(g)} \leftrightarrow Li_2CO_{3(s)} + Li_2SiO_{3(s)}\ \Delta E = 56\ \text{KJ/mol} \quad (2)$$

Kato and Nakagawa [37] used a thermogravimetric analyzer to determine the CO_2 absorption of Li_4SiO_4 in dry pure CO_2 gas with a flow rate of 300 ml/min. A clear weight increase was observed at approximately 720 °C. This weight change was approximately 35 mass%, which represents the amount of CO_2 absorption. In contrast with Li_4SiO_4, Li_2SiO_3 is non-sensitive to CO_2 capture in atmospheric air [39] and was a candidate air-exposure tolerant catalyst. Kato and Nakagawa [37] tested Li_2SiO_3 for the dry pure CO_2 capture, and observed no weight increase at temperatures up to 900 °C.

Li_2CO_3 species appeared in the FTIR spectrum of the catalyst (Fig. 3), indicating a favorable dispersion of a small amount of Li_2CO_3 on the catalyst surface. An interesting aspect from the FTIR results is that band vibrations of the Li_2CO_3 type bonds increased in intensity as the air-exposed time increased. This indicates an increase in the number of species over the catalyst surface. These results suggest the reaction of atmospheric CO_2 with catalyst. After exposure to air for 24–72 h, Li_2SiO_3 reacted with CO_2 in the air to form Li_2CO_3 over the catalyst surface. The basic strength (H_) of Li_2CO_3 stayed in the range of 9.8–15.0 even after exposure to air for 72 h. Therefore, only slight differences appeared in the soybean oil conversion between the air-exposed catalyst (24–72 h) (94.6–87.2%) and the fresh catalyst (97.0%). This implies that the catalytic

Table 1
Base strengths (H_) of as-prepared catalyst, CaO after exposing to air.

Exposure time (h)	Catalyst	Conversion[a]	CaO	Conversion[b]
0	15.0 < H_ < 18.4	97 ± 0.2	15.0 < H_ < 18.4	95
24	9.8 < H_ < 15.0	94.6 ± 0.6	7.2 < H_ < 9.8	3
48	9.8 < H_ < 15.0	93 ± 0.5	7.2 < H_ < 9.8	2
72	9.8 < H_ < ~15.0	87 ± 1.2	7.2 < H_ < 9.8	1
Reused	9.8 < H_ < 15.0	82 ± 2.3	N < H_ < A	N/A

[a] Reaction conditions: methanol to oil molar ratio = 12:1; catalyst amount = 4 wt.%; reaction temperature = 65 °C; reaction time = 3 h.
[b] Reaction conditions: methanol to oil molar ratio = 12:1; catalyst amount = 3 wt.%; reaction temperature = 65 °C; reaction time = 2 h.

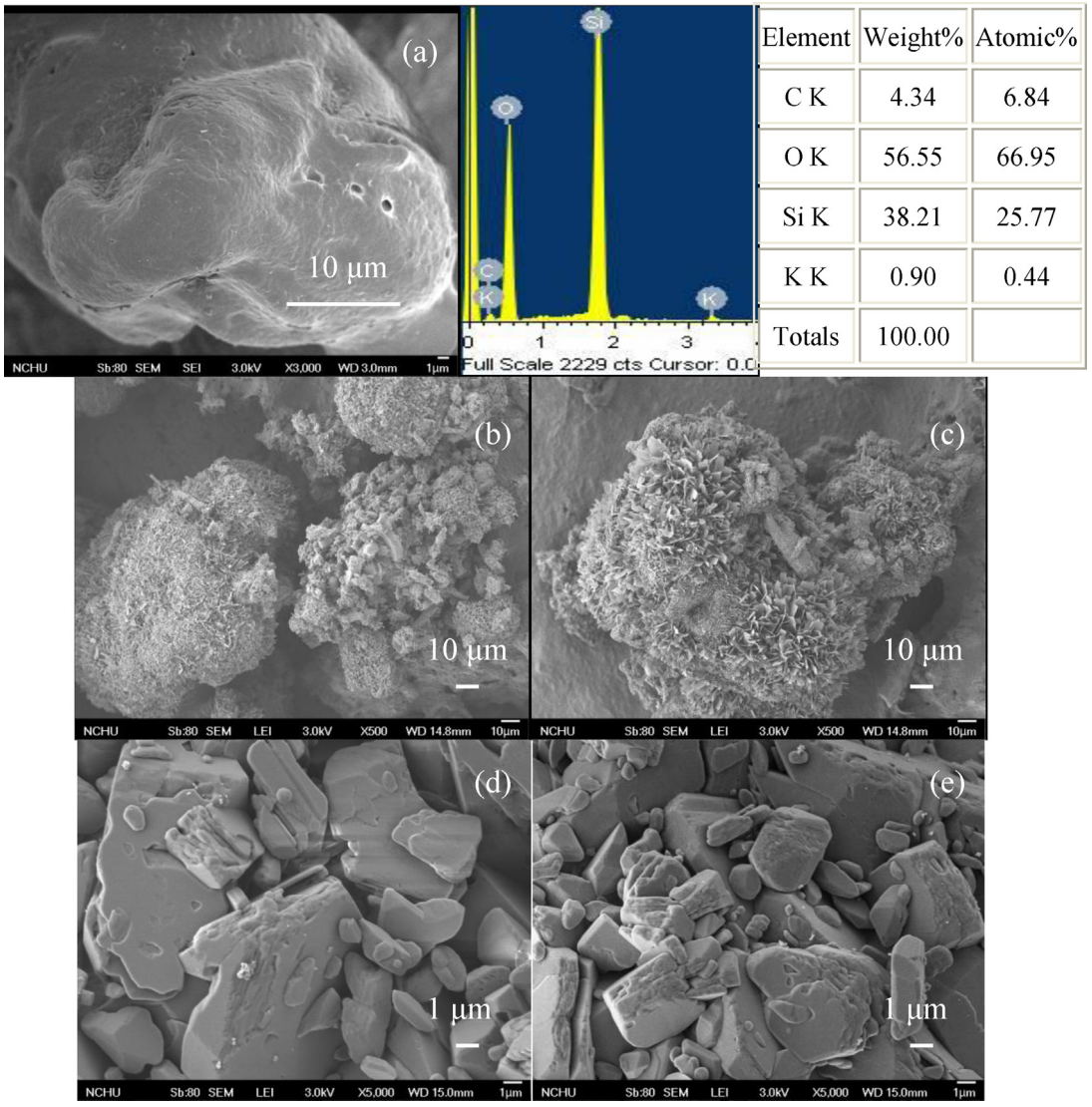

Element	Weight%	Atomic%
C K	4.34	6.84
O K	56.55	66.95
Si K	38.21	25.77
K K	0.90	0.44
Totals	100.00	

Fig. 4. (a) SEM morphology and EDS elemental analysis of RHA; SEM micrograph of (b) as-prepared catalyst, (c) catalyst exposure to air for 72 h, (d) fresh Li_2CO_3 and (e) Li_2CO_3 exposure to air for 72 h.

activity of the as-prepared catalyst was not seriously deactivated than CaO by carbonation in air on the catalyst surface. The XRD patterns (Fig. 2(b)) agree with this view, because the catalyst did not decompose to Li_2CO_3 and SiO_2 by absorbing CO_2 in the air at room temperature.

Fig. 4(a) presents SEM images of the RHA sample and the chemical composition of the ash determined by EDS. SEM micrographs of the rice husk ash indicated that the surface was spherical and impermeable porous in nature. Elemental composition with EDS showed that the SiO_2 was the main detected component, with a relatively low K content. Fig. 4(b) and (c) shows typical SEM images of the as-prepared catalyst and catalyst exposed to air for 72 h. All catalysts particles have an average grain size of approximately 50–100 μm. Many of the small particles with polyhedral crystals and flake cohered on the surface of catalyst. Fig. 4(d) and (e) also shows typical SEM images of the fresh Li_2CO_3 and Li_2CO_3 exposure to air for 72 h. Most Li_2CO_3 catalysts were in the form of irregular-shaped particles, with an average diameter of approximately 0.1–10 μm, and had impermeable porous surfaces. Results demonstrated that Li_2CO_3 catalytically tolerated exposure to air. This has important benefits when considering the industrial application of Li_2CO_3 as a solid catalyst, and the possibility of storing and handling the activated catalyst without taking special action to prevent contact with the ambient air.

Guo et al. used Na_2SiO_3 as an efficient solid base catalyst in the transesterification of soybean oil with methanol [40]. Na_2SiO_3 was hygroscopic and easy to deliquesce in the air [41]. In contrast to Na_2SiO_3, the Li_2SiO_3 catalyst in this study was a more anti-deliquescent catalyst in the air. The SEM patterns in Fig. 4 correspond with this view, because no further particle adhesion was apparent. This indicates that the as-prepared catalyst was not easily deliquesced in air for at least 72 h. Moreover, there were no obvious particles cohered on the surface of Li_2CO_3 after exposure to air for 72 h, implying that the deliquescent reaction in the air of the Li_2CO_3 on the surface of catalyst was also slight.

Ortiz *et al.* [35] used a TGA method to examine the hydration process of Li_4SiO_4 to elucidate water absorbed by Li_4SiO_4 particles. They reported that only approximately 0.045% (wt./wt. Li_4SiO_4) water adsorption on the Li_4SiO_4 surface was observed at 26 °C and 60% RH. In contrast with Li_4SiO_4, Li_2SiO_3 was non-sensitive to H_2O chemisorption in atmospheric air. Thermodynamic data show that the following reaction (3) do not occur spontaneously:

$$Li_2SiO_{3(s)} + H_2O_{(g)} \leftrightarrow 2LiOH_{(s)} + SiO_{2(s)}, \Delta G = 62.84\,KJ/mol \quad (3)$$

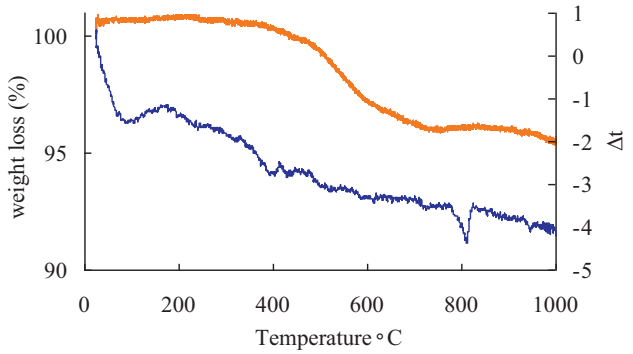

Fig. 5. TG-DTA curves for the catalyst exposure to air for 72 h.

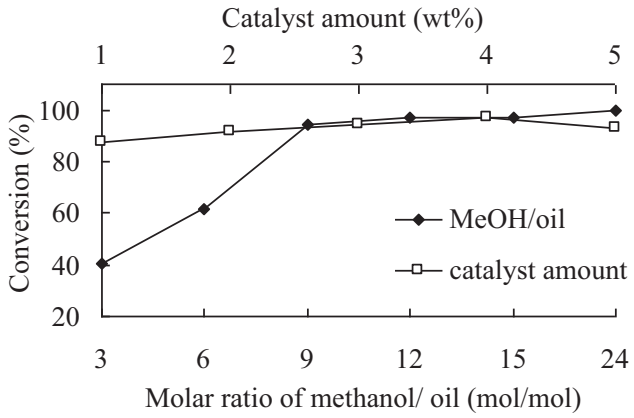

Fig. 6. Influence of catalyst amount (reaction conditions: 12.5 g soybean oil, methanol/oil molar ratio 12:1, reaction time 3 h, reaction temperature 65 °C) and methanol/oil molar ratio on the conversion (reaction conditions: 12.5 g soybean oil, catalyst amount 4 wt.%, reaction time 3 h, reaction temperature 65 °C).

This claim is supported by experimental results because the reaction was not observed (Figs. 2b and 3). Hashizume *et al.* (1997) examined the XRD patterns of Na-montmorillonite and NaCl at a relative humidity of 0–95%. They concluded that the crystal lattice of Na-montmorillonite and NaCl collapsed because of deliquescence. Fig. 1(b) shows that the crystal lattice of the as-prepared catalyst did not collapse after exposure to air for 24–72 h, indicating that there was no obvious deliquescent reaction on the catalyst surface. Absorbed water produces superficial hydroxylated species such as Si–OH and Li–OH between the Li_4SiO_4 and water vapor [35]. The FTIR spectrum of the as-prepared catalyst exposed to air (Fig. 3(b)) did not show OH stretching vibration (3562 cm^{-1}) and OH stretching vibrations of hydrogen-bonded (3530–2800) cm^{-1} [42], indicating that it was difficult for the as-prepared catalyst to chemisorb H_2O and transform to LiOH in the air.

The TGA curve for the as-prepared catalyst exposure to air for 72 h (Fig. 5) produced by the solid state method, showed that the initial reduction of weight occurred between room temperature and 100 °C. This weight loss was attributed to an evaporation process for H_2O physisorption. A second weight loss of 4.7% between 450 and 750 °C, which is due to a decarbonation process, appears between 450 and 650 °C [43]. It might also be the result of complicated reactions between the lithium compounds and silicon compounds [44], which might be divided into two steps [45]:

$$515-565\,^{\circ}C: Li_2CO_3 + SiO_2 \rightarrow Li_2SiO_3 + CO_2$$
$$565-730\,^{\circ}C: Li_2CO_3 + SiO_2 \rightarrow Li_2SiO_3 + CO_2$$

and then

$$Li_2SiO_3 + Li_2CO_3 \rightarrow Li_4SiO_4 + CO_2 \quad (4)$$

XRD analyses did not show the presence of impurities (Li_2CO_3 and SiO_2), which might form after the experiment from a decomposition reaction of Li_4SiO_4 with moisture and CO_2 in the air. However, thermal analyses demonstrated that both materials contained some minor impurities. Note that the lower detection limit of the XRD technique depends on the scattering properties of the components of the materials. Silicates are typically detected when the concentration is higher than 3% and the crystal is bigger than 3 nm [43]. After the second change, the weight kept decreasing slowly with an endothermic signal, showing the vaporization of $Li_2O_{(s)}$ can easily occur [46].

3.2. Transesterification reaction condition optimization

This study also investigates the effects of catalyst amount on conversion. The catalyst amount varied from 1 to 5% (catalyst/oil weight ratio). As Fig. 6, the conversion increased as the catalyst amount increased from 1 to 4%. The conversion reached a plateau value at the catalyst weight percentage between 4 and 5%. Additional catalysts increased the contact opportunity of the catalyst and the reactant, directly influencing the reaction speed and the conversion. Mass transfer and reactant adsorption on the catalyst are crucial in heterogeneous catalysis [47–49]. Therefore, a molar ratio higher than the stoichiometric molar ratio of methanol is required to shift the equilibrium for the reaction. As Fig. 6 shows, conversion increased considerably with an increase in the methanol-loading amount. The maximal conversion ratio was 99.5% at the methanol/oil molar ratio of 24:1. Fig. 7 displays the effects of reaction time and reaction temperature on conversion. More than 93.0% of the conversion can occur within 1 h reaction time, and thereafter remained nearly constant as a result of a nearly equilibrium conversion. Four different temperatures were used for the transesterification of refined soybean oil with methanol (12:1) using 4 wt.% catalyst. After 3 h, conversions were 97.0, 86.7, 51.5, and 19.9% for 65, 50, 40, and 30 °C, respectively. Temperature clearly influenced the reaction rate and the biodiesel purity.

After the transesterification was completed, the samples were recovered using simple decantation. The remaining catalyst in the reactor was used to catalyze the next batch of transesterification. A biodiesel purity of 86.7% could be obtained even after recycling the

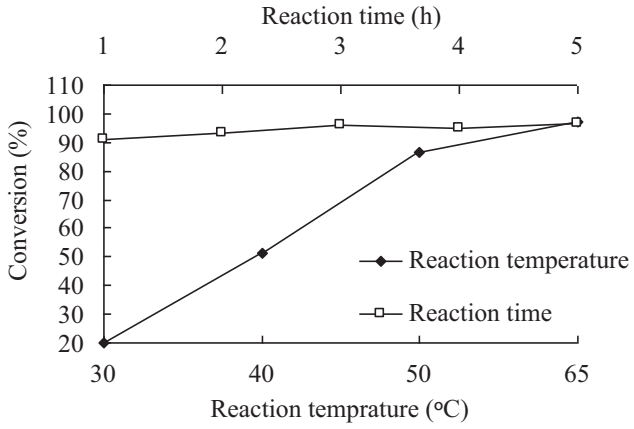

Fig. 7. Influence of reaction time (reaction conditions: 12.5 g soybean oil, methanol/oil molar ratio 12:1, catalyst amount 4 wt.%, reaction temperature 65 °C) and reaction temperature on the conversion (reaction conditions: 12.5 g soybean oil, methanol/oil molar ratio 12:1, catalyst amount 4 wt.%, reaction time 3 h).

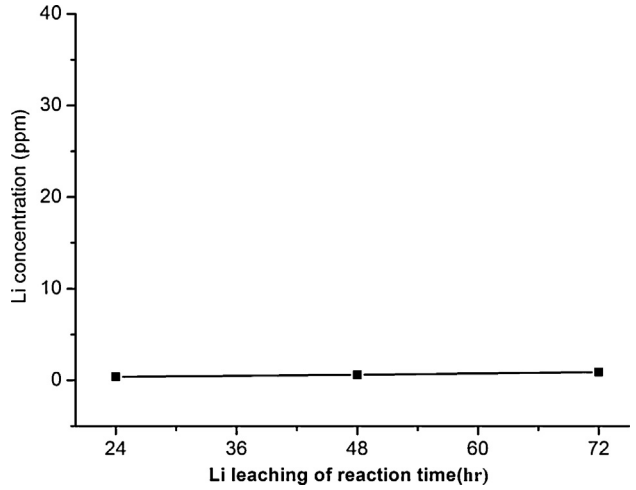

Fig. 8. The Li leaching of reaction time (reaction conditions: 12.5 g soybean oil, methanol/oil molar ratio 12:1, catalyst amount 4 wt.%, reaction temperature 65 °C).

catalyst 5 times. Because the amount of catalyst used in the next run was lower than the initial run, which might partly be responsible to the reduced biodiesel purity during the subsequent run. Glycerol covering the surface of catalyst was another possible reason for activity loss. Among the alkali and alkali earth oxides, CaO is one of the solids that have displayed higher transesterification activity (Granados *et al*., 2007). The glycerol released during the transesterification reaction reacts with CaO to form Ca glyceroxides [29]. In the present study, the crystalline phase of the catalyst remained unchanged (Fig. 1(b)) after catalyst regeneration. This indicates that the catalyst has greater stability than CaO in the transesterification reaction, but its lifetime in an industrial setting must be significantly prolonged to be practical.

The solubility of the catalysts is another critical factor to accurately interpret their performance and assess their potential practical applications. This is a significant issue because the presence of metal necessitates neutralization and washing steps in the production process, thus nullifying the possible advantage of using these compounds as heterogeneous catalysts. The first transesterification reaction produced FAME containing 0.4 ppm of lithium. Fig. 8 shows that concentration of Li^+ under different using times were all below the 1 ppm. These results demonstrate extremely small quantities (free Li^+ concentration of less than 1 ppm) in the biodiesel. These results indicate that the as-prepared catalyst was suitable for use in biodiesel production from soybean oil. The main advantage of the solid base catalyst is that it can be used repeatedly. Fig. 9 shows that RHA reprocessing as a silica source to synthesize a Li_2SiO_3 catalyst exhibiters a fairly good operational stability, *i.e.*, 94% of the conversion for the first reaction and 86% of the conversion is retained for the fifth reaction. It clearly indicates the advantage of solid base catalyst for reaction stability and the possible feasibility can be enhanced in industrial production.

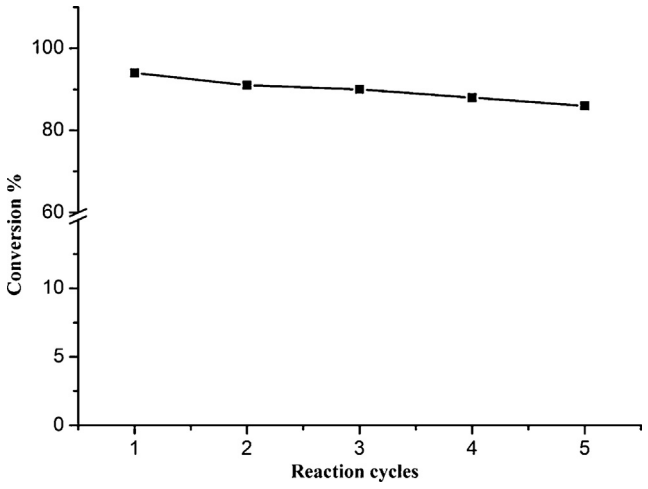

Fig. 9. Reusability study after five reaction cycles for catalyst (reaction conditions: catalyst amount 4 wt.%, methanol/oil molar ratio 12:1, reaction time 4 h, reaction temperature 65 °C).

4. Conclusions

This study revealed RHA reprocessing as a silica source to synthesize a Li_2SiO_3 catalyst for possible applications in biodiesel production. Experimental results show that as-prepared catalyst demonstrated excellent catalytic activity because of its basic strength (H_), above 15.0. In many base-catalyzed reactions, solid base catalysts are easily poisoned by carbon dioxide and water. The as-prepared catalyst is tolerant to water and carbon dioxide and the catalytic activity of transesterification reactions were not significantly lower because no obvious LiOH formed on the catalyst surface and Li_2CO_3 was yet an efficient solid base catalyst ($H_- > 9.8$). It clearly indicates the advantage of solid base catalyst for reaction stability and the possible feasibility can be enhanced in industrial production.

Acknowledgment

The authors thank NSC Taiwan for financially supporting this study under grant NSC100–2622-M-42–001-CC1.

References

[1] Tang S, Wang L, Zhang Y, Tian S, Wang B. Study on preparation of Ca/Al/Fe_3O_4 magnetic composite solid catalyst and its application in biodiesel transesterification. Fuel Process Technol 2012;95:84–9.
[2] Kaur MD, Ali AJ. Lithium ion impregnated calcium oxide as nano catalyst for the biodiesel production from karanja and jatropha oils. Renew Energy 2011;36:2866–71.
[3] Kaur MD, Ali AJ. Nanocrystalline lithium ion impregnated calcium oxide as heterogeneous catalyst for transesterification of high moisture containing cotton seed oil. Energy Fuels 2010;24:2091–7.
[4] Fan M, Zhang P, Ma Q. Enhancement of biodiesel synthesis from soybean oil by potassium fluoride modification of a calcium magnesium oxides catalyst. Bioresour Technol 2012;104:447–50.
[5] Jairam S, Kolar P, Sharma-Shivappa R, Osborne JA, Davis JP. Ki-impregnated oyster shell as a solid catalyst for soybean oil transesterification. Bioresour Technol 2012;104:329–35.
[6] Nakatani N, Takamori H, Takeda K, Sakugawa H. Transesterification of soybean oil using combusted oyster shell waste as a catalyst. Bioresour Technol 2009;100:1510–3.
[7] Boro J, Thakur AJ, Deka D. Solid oxide derived from waste shells of turbonilla striatula as a renewable catalyst for biodiesel production. Fuel Process Technol 2011;92:2061–7.
[8] Boey PL, Maniam GP, Hamid SA, Ali DMH. Utilization of waste cockle shell (*Anadara granosa*) in biodiesel production from palm olein: optimization using response surface methodology. Fuel 2011;90:2353–8.
[9] Hu S, Wang Y, Han H. Utilization of waste freshwater mussel shell as an economic catalyst for biodiesel production. Biomass Bioenergy 2011;35:3627–35.
[10] Viriya Empikul N, Krasae P, Puttasawat B, Yoosuk B, Chollacoop N, Faungnawakij K. Waste shells of mollusk and egg as biodiesel production catalysts. Bioresour Technol 2010;101:3765–7.
[11] Cho YB, Seo G. High activity of acid-treated quail eggshell catalysts in the transesterification of palm oil with methanol. Bioresour Technol 2010;101:8515–9.
[12] Boey P-L, Maniam GP, Hamid S-A. Biodiesel production via transesterification of palm olein using waste mud crab (*Scylla serrata*) shell as a heterogeneous catalyst. Bioresour Technol 2009;100:6362–8.
[13] Nair P, Singh B, Upadhyay SN, Sharma YC. Synthesis of biodiesel from low Ffa waste frying oil using calcium oxide derived from mereterix mereterix as a heterogeneous catalyst. J Cleaner Prod 2012;29–30:82–90.

[14] Birla A, Singh B, Upadhyay SN, Sharma YC. Kinetics studies of synthesis of biodiesel from waste frying oil using a heterogeneous catalyst derived from snail shell. Bioresour Technol 2012;106:95–100.
[15] Memon SA, Shaikh MA, Akbar H. Utilization of rice husk ash as viscosity modifying agent in self compacting concrete. Constr Build Mater 2011;25:1044–8.
[16] Armesto L, Bahillo A, Veijonen K, Cabanillas A, Otero J. Combustion behaviour of rice husk in a bubbling fluidised bed. Biomass Bioenergy 2002;23:171–9.
[17] Mane VS, Deo Mall I, Chandra Srivastava V. Kinetic and equilibrium isotherm studies for the adsorptive removal of brilliant green dye from aqueous solution by rice husk ash. J Environ Manage 2007;84:390–400.
[18] Fuad MYA, Ismail Z, Ishak ZaM, Omar AKM. Application of rice husk ash as fillers in polypropylene: effect of titanate, zirconate and silane coupling agents. Eur Polym J 1995;31:885–93.
[19] Zerbino R, Giaccio G, Isaia GC. Concrete incorporating rice-husk ash without processing. Constr Build Mater 2011;25:371–8.
[20] Krishnarao RV, Subrahmanyam J, Jagadish Kumar T. Studies on the formation of black particles in rice husk silica ash. J Eur Ceram Soc 2001;21:99–104.
[21] Prasetyoko D, Ramli Z, Endud S, Hamdan H, Sulikowski B. Conversion of rice husk ash to zeolite beta. Waste Manage 2006;26:1173–9.
[22] Zain MFM, Islam MN, Mahmud F, Jamil M. Production of rice husk ash for use in concrete as a supplementary cementitious material. Constr Build Mate 2011;25:798–805.
[23] Chowdhury S, Mishra R, Saha P, Kushwaha P. Adsorption thermodynamics kinetics and isosteric heat of adsorption of malachite green onto chemically modified rice husk. Desalination 2011;265:159–68.
[24] Vieira MGA, Neto AFDA, Silva MGCD, Carneiro CN, Filho AaM. Influence of the system on adsorption of Pb(II) and Cu(II) by rice husks ash: kinetic study. Chem Eng Trans 2011;24:1213–8.
[25] Othman Ali I, Hassan AM, Shaaban SM, Soliman KS. Synthesis and characterization of Zsm-5 zeolite from rice husk ash and their adsorption of Pb^{2+} onto unmodified and surfactant-modified zeolite. Sep Purif Technol 2011;83:38–44.
[26] An D, Guo Y, Zou B, Zhu Y, Wang Z. A study on the consecutive preparation of silica powders and active carbon from rice husk ash. Biomass Bioenergy 2011;35:1227–34.
[27] Wang K, Guo X, Zhao P, Wang F, Zheng C. High temperature capture of CO_2 on lithium-based sorbents from rice husk ash. J Hazard Mater 2011;189:301–7.
[28] Saceda J-JF, Leon RLD, Rintramee K, Prayoonpokarach S, Wittayakun J. Properties of silica from rice husk and rice husk ash and their utilization for zeolite Y synthesis. Quim Nova 2011;34:1394–7.
[29] Wang JX, Chen KT, Wen BZ, Liao YH, Chen CC. Transesterification of soybean oil to biodiesel using cement as a solid base catalyst. J Taiwan Inst Chem Eng 2012;43:215–9.
[30] Granados ML, Poves MDZ, Alonso DM, Mariscal R, Galisteo FC, Moreno-Tost R, et al. Biodiesel from sunflower oil by using activated calcium oxide. Appl Catal B-Environ 2007;73:317–26.
[31] Granados ML, Alba-Rubio AC, Vila F, Martín Alonso D, Mariscal R. Surface chemical promotion of Ca oxide catalysts in biodiesel production reaction by the addition of monoglycerides diglycerides and glycerol. J Catal 2010;276:229–36.
[32] Arzamendi G, Arguiñarena E, Campo I, Zabala S, Gandía LM. Alkaline and alkaline-earth metals compounds as catalysts for the methanolysis of sunflower oil. Catal Today 2008;133–135:305–13.
[33] Kouzu M, Yamanaka SY, Hidaka JS, Tsunomori M. Heterogeneous catalysis of calcium oxide used for transesterification of soybean oil with refluxing methanol. App Catal A-Gen 2009;355:94–9.
[34] Ortiz LJ, Contreras García ME, Gómez Yáñez C, Pfeiffer H. Surfactant-assisted hydrothermal crystallization of nanostructured lithium metasilicate (Li_2SiO_3) hollow spheres: (I) synthesis, structural and microstructural characterization. J Solid State Chem 2011;184:1304–11.
[35] Ortiz LJ, Martínez DL, Gómez Yáñez C, Pfeiffer H. Towards understanding the thermoanalysis of water sorption on lithium orthosilicate (Li_4SiO_4). Thermochim Acta 2011;515:73–8.
[36] Kouzu M, Tsunomori M, Yamanaka S, Hidaka J. Solid base catalysis of calcium oxide for a reaction to convert vegetable oil into biodiesel. Adv Powder Technol 2010;21:488–94.
[37] Kato M, Nakagawa K. New series of lithium containing complex oxides, lithium silicates, for application as a high temperature CO_2 absorbent. J Ceram Soc Jpn 2001;109:911–4.
[38] Khomane RB, Sharma BK, Saha S, Kulkarni BD. Reverse microemulsion mediated sol–gel synthesis of lithium silicate nanoparticles under ambient conditions: scope for CO_2 sequestration. Chem Eng Sci 2006;61:3415–8.
[39] Rodríguez MT, Pfeiffer H. Sodium metasilicate (Na_2SiO_3): a thermo-kinetic analysis of its CO_2 chemical sorption. Thermochim Acta 2008;473:92–5.
[40] Guo F, Peng ZG, Dai JY, Xiu ZL. Calcined sodium silicate as solid base catalyst for biodiesel production. Fuel Process Technol 2010;91:322–8.
[41] George AM, Richet P, Stebbins JF. Cation dynamics and premelting in lithium metasilicate (Li_2SiO_3) and sodium metasilicate (Na_2SiO_3): a high-temperature NMR study. Am Mineral 1998;83:1277–84.
[42] Maiti GC, Baerns M. Dehydration of sodium hydroxide and lithium hydroxide dispersed over calcium oxide catalysts for the oxidative coupling of methane. Appl Catal A-Gen 1995;127:219–32.
[43] Cruz D, Bulbulian S, Lima E, Pfeiffer H. Kinetic analysis of the thermal stability of lithium silicates (Li_4SiO_4 and Li_2SiO_3). J Solid State Chem 2006;179:909–16.
[44] Li XQ, Guo HJ, Li LM, Li XH, Wang ZX, Ou H, et al. Effects of calcination temperature on properties of Li_2SiO_3 for precursor of Li_2FeSiO_4. Trans Nonferr Met Soc 2011;21:529–34.
[45] Tang T, Zhang Z, Meng J-B, Luo D-L. Synthesis and characterization of lithium silicate powders. Fusion Eng Des 2009;84:2124–30.
[46] Noda S, Nishioka M, Sadakata M. Gas-phase hydroxyl radical emission in the thermal decomposition of lithium hydroxide. J Phy Chem B 1999;103:1954–9.
[47] Wang J, Chen K, Chen C. Biodiesel production from soybean oil catalyzed by K_2SiO_3/C. Chin J Catal 2011;32:1592–6.
[48] Chen YH, Huang YH, Lin RH, Shang NC, Chang CY, Chang CC, et al. Biodiesel production in a rotating packed bed using K/gamma-Al_2O_3 solid catalyst. J Taiwan Inst Chem Eng 2011;42:937–44.
[49] Manh DV, Chen YH, Chang CC, Chang MC, Chang CY. Biodiesel production from Tung oil and blended oil via ultrasonic transesterification process. J Taiwan Inst of Chem Eng 2011;42:640–4.